Biomaterials Translational

Hyaluronic acid-based hydrogels with tobacco mosaic virus containing cell adhesive peptide induce bone repair in normal and osteoporotic rats

Jishan Yuan[1], Panita Maturavongsadit[2,3], Zhihui Zhou[1], Bin Lv[1], Yuan Lin[4], Jia Yang[2], Jittima Amie Luckanagul[5,6,]*

Key Words:
bone regeneration; calvarial defect; hydrogel; osteoporosis; tobacco mosaic virus

From the Contents

ABSTRACT

Tobacco mosaic virus (TMV) has been studied as a multi-functional agent for bone tissue engineering. An osteo-inductive effect of wild-type TMV has been reported, as it can significantly enhance the bone differentiation potential of bone marrow stromal cells both on a two-dimensional substrate and in a three-dimensional (3D) hydrogel system. A TMV mutant (TMV-RGD1) was created which featured the adhesion peptide arginyl-glycyl-aspartic acid (RGD), the most common peptide motif responsible for cell adhesion to the extracellular matrix, on the surface of the virus particle to enhance the bio-functionality of the scaffold material. We hypothesised that the incorporation of either wild-type TMV or TMV-RGD1 in the 3D hydrogel scaffold would induce bone healing in critical size defects of the cranial segmental bone. We have previously tested the virus-functionalised scaffolds, in vitro, with a hyaluronic acid-based system as an in-situ hydrogel platform for 3D cell encapsulation, culture, and differentiation. The results of these experiments suggested the potential of the virus-functionalised hydrogel to promote in vitro stem cell differentiation. The hydrogel-forming system we employed was shown to be safe and biocompatible in vivo. Here, we further explored the physiological responses regarding bone regeneration of a calvarial defect in both normal and osteoporotic ovariectomized rat models. Our results, based on histological analysis in both animal models, suggested that both wild-type TMV and TMV-RGD1 functionalised hydrogels could accelerate bone regeneration, without systemic toxicity, evaluated by blood counts. New bone formation was intensified by the incorporation of the RGD-mutant viral particles. This finding increased the potential for use of the rod-shaped plant virus as a platform for the addition of powerful biofunctionality for tissue engineering applications. This study was approved by the Ethics Committee on Animal Use of the Zhenjiang Affiliated First People's Hospital affiliated to Jiangsu University.

***Corresponding authors:**
Jittima Amie Luckanagul,
jittima.luck@gmail.com.

http://doi.org/10.3877/cma.j.issn.2096-112X.2020.01.009

How to cite this article:
Yuan, J.; Maturavongsadit, P.; Zhou, Z.; Lv, B.; Lin, Y.; Yang, J.; Luckanagul, J. Hyaluronic acid-based hydrogels with tobacco mosaic virus containing cell adhesive peptide induce bone repair in normal and osteoporotic rats. *Biomater Transl.* **2020**, *1*(1), 89-98.

Introduction

The surprising discovery, first reported in 2008, that tobacco mosaic virus (TMV) accelerates bone differentiation of mesenchymal stem cells (MSCs), and curiosity regarding this effect, have been inspiring extensive research in our group.[1-7] We demonstrated that a TMV substrate promoted MSC osteogenesis by upregulating bone morphogenetic protein-2 (BMP-2) gene expression.[4, 5] With the well-known clinically-proven role of BMP-2 in bone repair, and the discovery that it is highly upregulated on a two-dimensional virus-coated cell culture surface, the search was on for more clinically-compliant three-dimensional (3D) systems incorporating the virus and its bio-functional derivatives which could be designed and tested for tissue engineering applications.[3, 6, 7] 3D hydrogels provide an excellent environment for cell–cell and cell–matrix interaction. Moreover, hydrogel systems can be directly used in subsequent tissue-engineering applications. Owing to the hydrophilic polymer network with high water content, and solid-like mechanical properties, hydrogels can be ideal systems for providing a tailored microenvironment supporting microvasculature and tissue growth.[8-12] In addition, the exchange of electrolytes, small molecules and cytokines along with cell migration are allowed by the porous structure that is essential for cell viability and tissue growth.[13, 14] A hydrogel system must be able to accommodate and present bio-functionality synergising desirable physical, chemical, and cell-responsive properties to serve different biomedical applications.[15, 16]

We have previously reported our creation of a porous sponge-like scaffold based on alginate hydrogel pre-cast with TMV and its mutant RGD (TMV-RGD) for enhanced osteogenesis of 3D-cultured MSCs.[17] In addition, we have created a hybrid TMV scaffold in a simple injectable form, using thiol-ene "click" chemistry, to promote the differentiation of MSCs to cartilage.[3] Methacrylated hyaluronic acid (MeHA) polymer was cross-linked with cysteine-inserted TMV mutants (TMV1cys) through thiol-ene reaction, with the hydrogel structured under physiological conditions. Using this TMV–hydrogel hybrid system as 3D scaffold, enhanced collagen accumulation and BMP-2 upregulation were observed, resulting in promotion of the *in vitro* chondrogenesis of MSCs. In another model hydrogel scaffold, incorporation of RGD-inserted TMV mutants (TMV-RGD) into the polysaccharide-based hydrogel further promoted the *in vitro* differentiation of BMSCs, while also demonstrating an increase in collagen production.[17] These results suggested that TMV and TMV-RGD could play critical roles in directing MSC chondrogenesis in a hydrogel microenvironment.

These continuing efforts have been focusing on a pre-clinical series of *in vivo* studies. We have tested the effects of TMV and TMV-RGD mutant in a 3D sponge-like alginate hydrogel based on their toxicity in both mouse and rat models and their efficacy regarding bone regeneration potential in a cranial defect rat model. TMV, as a plant virus nano-scaffolding material, might have raised concerns regarding its effect on the humoral immune response, which could be a potential drawback of using plant virus materials in clinical tissue-engineering applications. The antigenicity of TMV and its RGD mutant in the hydrogel implant was evaluated and the results demonstrated that the virus was biocompatible in the form of a hydrogel implant using a BALB/c mouse model. Immune response towards TMV was compromised by the immobilisation and slow release of the virus from the bulk hydrogels.[18] In another study using normal rat model with cranial bone removal, inflammation and healing of confined critical size cranial bone defects when treated with porous alginate hydrogels carrying TMV and TMV-RGD were comparatively investigated. Both types of scaffolds permitted the healing of critical size defects (CSDs) in the cranial segmental bone and demonstrated superiority in bone remodelling and maturation compared to the blank carrier control, as shown by histological data.[19] In correlation with the mouse model, no systemic inflammatory reactions nor severe immunogenic adverse effects were observed.[18]

Hyaluronic acid (HA) is a polysaccharide commonly found in the human body which is a component of the connective tissue microenvironment important for cell survival, motility, differentiation and proliferation. It has many biological roles in the body such as tissue organisation, wound healing, and angiogenesis. HA is a linear chain polysaccharide composed of repeating disaccharides, glucuronic acid and N-acetylglucosamine. HA possesses negative charges that can attract water molecules conferring the ability to form hydrogels suitable as extracellular matrix surrogates. One of the most interesting polymer-based delivery systems, which can form gels after application to the delivery site, is the "*in situ* gel system". Such a system can also offer a variety of mechanical features similar to a solid-like material, but, on the other hand, can be administered in a liquid form that could be beneficial for clinical operation.[20] With this *in situ* gel character, the system allows simultaneous incorporation of other therapeutics such as proteins, cytokines, nanoparticles, and cells, for which personalised dosing may be critical during the administration operation. Moreover, the material has the potential to fill the irregular spaces of a defect area. The sol-to-gel transition of an *in situ* gel can be induced by various mechanisms, for example; ultraviolet light is one popular example of a stimulant for *in situ* photo-crosslinking of hydrogels. We here utilised a hydrogel carrier system with a chemical trigger. The sol-to-gel transition occurs at a pre-defined time after the chemical crosslinker is added into the formulation mixture containing modified HA as the gel-forming polymer. This system has been well-characterised *in vitro* in terms of its physical properties, microstructure, mechanical properties, and cyto-compatibility. This hydrogel formulation was developed from medium molecular weight HA, modified with a methacrylate group, as a major scaffold component of the hydrogel. The *in situ* crosslinking with dithiothreitol was induced via a Michael addition reaction under physiological conditions.[21, 22] Gelation time, porosity and mechanical properties of the hydrogel can be tailored by altering the degree of modification of HA (methacrylation of HA), the concentration of HA, and the ratio of crosslinkers.[23] However, for our proof-of-concept study focusing on the *in vivo* efficacy of the TMV and TMV-RGD incorporated into an HA hydrogel carrier for use in bone repair, the *in situ* gel was pre-cast in a mould and implanted into the defect site.

Osteoporosis can be caused by many factors with multiple gene interactions. Patients with this non-communicable disease are prone to suffer fragility fractures of vertebrae, hips and radii. A critical concern for this group of patients is the complications, which they can experience following serious fractures that may occur due to accidents and trauma. The delays in healing, regeneration and recovery can be significant due to aging and the pre-existing genetic background. The public apprehension of disease is tremendous and continuously growing, globally, while average life expectancy is also on the upsurge. The clinical need for bone repair, systemic or locally-induced bone regeneration and bone tissue engineering has increased and become a challenge for health-care systems.[24] A study suggested that osteoporosis is a major problem contributing to the increasing cost of medical care in the European Union in which mortality and morbidity rates are rising in the elderly with the disease. The incidence of osteoporotic fractures is higher in women compared to men, since women after menopause experience hormonal alterations which can cause a serious loss of bone mass.[25] One of the most commonly-used animal models in research on postmenopausal

1 Department of Orthopaedic Surgery, the Affiliated First People's Hospital to Jiangsu University, Zhenjiang, Jiangsu Province, China; 2 Department of Chemistry and Biochemistry, University of South Carolina, Columbia, SC, USA; 3 Joint Department of Biomedical Engineering, North Carolina State University and The University of North Carolina at Chapel Hill, Chapel Hill, NC, USA; 4 The State Key Laboratory of Polymer Physics and Chemistry, Changchun Institute of Applied Chemistry, Chinese Academy of Sciences, Changchun, Jilin Province, China; 5 Department of Pharmaceutics and Industrial Pharmacy, Faculty of Pharmaceutical Sciences, Chulalongkorn University, Bangkok, Thailand; 6 Research Unit for Plant-produced Pharmaceuticals, Chulalongkorn University, Bangkok, Thailand.

osteoporosis is the ovariectomised (OVX) rat model. It has been evidenced that statistically-significant bone loss is observed in the proximal tibial metaphysis in just 14 days after the OVX induction of normal rats. When rats were subjected to ovary removal, bone resorption exceeded bone formation initially, causing bone loss. After a certain period, bone remodelling eventually reached a steady state, with a balance between resorption and formation, for example; a 90-day interval was required for the proximal tibial metaphysis to reach a steady state.[26, 27] In this report, we explored the effect of TMV and its RGD mutant embedded within an *in situ* HA-based hydrogel on bone regeneration in both normal and osteoporotic model rats as shown in **Figure 1**.

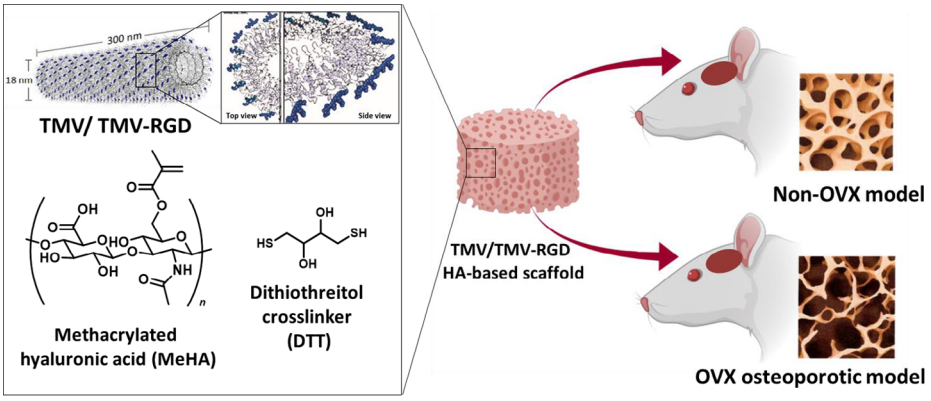

Figure 1. Schematic illustration of our study design. Methacrylated hyaluronic acid (MeHA) was synthesised and used with incorporated virus particles as a hydrogel structural platform to fill skull defects in osteoporotic and normal Sprague-Dawley rats. The RGD mutant TMV graphic was generated from PyMol with coordinates 2TMV from the Protein Data Bank (www.rcsb.org) and created with BioRender.com. OVX: ovariectomised; RGD: arginyl-glycyl-aspartic acid; TMV: tobacco mosaic virus.

Methods

Preparation of virus-functionalised MeHA hydrogel and synthesis of MeHA

MeHA was synthesized following the published protocol.[3] In this study, HA with molecular weight between 40–60 kDa was used. The reaction was one step and was carried out at a pH maintained above 8.0. Methacrylate anhydride was added twice during the entire process. Briefly, HA was dissolved at 1 wt% in potassium phosphate buffer, pH 8, and methacrylic anhydride, at a 6- to 10-fold molar excess relative to the HA disaccharide repeat unit, was added dropwise to the solution at 4°C. The pH of the two-phase reaction mixture was adjusted to 8.0 with 5 M aqueous NaOH, and the reaction was continued for 24 hours at 4°C with frequent readjustment of the solution pH to keep it above 8.0. The product was dialyzed against milli-Q water for at least 48 hours, followed by centrifugation to obtain the precipitate, which was then flash-frozen in liquid nitrogen and then lyophilised, resulting in a dry product that was further analysed and the degree of modification calculated by proton nuclear magnetic resonance. The expected degree of modification was 40–50% of total functional HA monomer molecules.

Hydrogel fabrication and functionalisation with virus particles

In general, to fabricate the HA hydrogels, MeHA polymers with a degree of modification of 40–50% were dissolved in phosphate-buffered saline at a concentration of 3 wt%, followed by the cross-linking agent, dithiothreitol, that was added at a molar ratio of thiol/ene = 2:1. The pH of the mixture was adjusted to 8.0 with 2 M aqueous NaOH, and gelation took place at the predicted time. To form the TMV-based HA hydrogels, the same procedure was adopted with incorporation of wild-type TMV or TMV-RGD mutant suspended in potassium phosphate buffer to make a final virus concentration of 0.1 wt% in the pre-gel solution before the addition of dithiothreitol.

Animals, experimental design and treatments

The animal model protocols of this study were approved by the Ethics Committee on Animal Use of the Zhenjiang Affiliated First People's Hospital affiliated to Jiangsu University. Twelve-week-old female Sprague-Dawley rats were purchased from Cavens (Changzhou, China). Twenty-four rats were randomly divided into an osteoporosis group, in which osteoporosis was established by ovariectomy (OVX group), and a normal group, with twelve rats in each group. The OVX surgery was carried out using the same procedure as previously described in a mouse model.[28, 29] Briefly, rats were anesthetised with 1% pentobarbital (40 mg/kg). then placed in a prone position on a fixed table, and the limbs and head were fixed. Conventional skin preparation was conducted with a 1.5 cm radius, the operative area was disinfected, and covered with sterile drapes. A 1.5 cm dorsal incision was made at the posterior midline of the back with a scalpel, below the costal margin of both sides as the centre, and below the costal margin of both sides as the radius. After ligation, complete removal of the ovary was confirmed by careful observation and the animal was checked for any bleeding in the uterine horn. After dressing, the muscle and fascia were sutured, then the skin was closed using discontinuous sutures. The contralateral ovary was excised in the same way and the wound was closed. Sham operation of the control group was performed following the same procedure as that of the experimental group, but the ovary was preserved and adipose tissue around the ovary of equal weight was removed.

At 12 weeks post-OVX, a skull defect 8 mm in diameter was created in all animals. Within each group (normal and OVX groups), three rats were treated as a mock group without hydrogel treatment, while the remaining nine rats constituted the treatment groups. In the treatment groups, each rat was randomly assigned to treatment with one of three different types of hydrogel (n = 3 per treatment) to replace the defect. The hydrogels were: 1) blank MeHA, 2) wild-type TMV-incorporated MeHA, and 3) TMV-RGD mutant-incorporated MeHA.

Disk-shaped hydrogels were implanted to fill the cranial bone defects generated. Rats were given 2–4 mg/kg of subcutaneous carprofen 2–4 hours before surgery for analgesia. Procaine penicillin (60,000 IU) was given subcutaneously for infection prophylaxis. Instruments were autoclaved prior to use to minimise the risk of post-surgical infection and cross-contamination. The animals were anesthetised with 3% isoflurane in oxygen. After the appropriate level of anaesthesia was obtained, the fur over the cranium was shaved, and the skin was cleansed with normal saline to remove loose hair. A dry heating pad was used to maintain the animal's body temperature during surgery. A midline incision was made from the middle of the nasofrontal area to the external occipital protuberance utilising a sterile No. 15 scalpel blade. Full-thickness skin flaps were reflected laterally with a periosteal elevator to expose the calvaria. An 8-mm craniotomy was performed in all animals utilising a dental handpiece system at low speed and with copious sterile saline irrigation to remove loose debris and to avoid the generation of frictional heat at the surgical site. The bone defects were standardised using an 8-mm diameter trephine bur to outline the treatment area. A PTFE barrier membrane (kindly provided by Osteogenics Biomedical, Lubbock, TX, USA) was inserted to form a barrier on top of the dura. Each hydrogel was carefully placed into the defect, and a second PTFE membrane was placed over the defect and under the periosteum. The periosteum was repositioned and the defect was then closed with continuous interlocking sutures using nylon suture material. Postoperative analgesia to relieve pain (carprofen, 2–4 mg/kg) was given orally at least once every 24 hours for 48 hours. The animals were weighed before and after surgery then daily for the first 2 days and weekly until the end of the experiment. Signs of pain or distress were monitored daily after surgery.

Haematological assay

A complete blood count was performed immediately after each blood withdrawal. A 20 μL blood sample was transferred into a 1 mL microtainer tube with dipotassium ethylenediamine tetraacetic acid. Each tube was analysed in an automated blood counter machine (Shanghai Jill Biochemical Co. Ltd., Shanghai, China). The numbers of total white blood cells, haemoglobin, lymphocytes (LYM), mean platelet volume (MPV), monocytes (MON), neutrophils, platelets and red blood cells were evaluated.

Histological analysis

The cranial tissues of the experimental group and the control group were collected and fixed in 10% formalin. The treated tissue was embedded in paraffin and 5 μm paraffin sections were prepared. Hematoxylin and eosin (H&E) and Masson's trichrome staining were then performed on the tissue sections following standard procedures. The degree of tissue inflammation was graded as 0, 1, 2, or 3 according to the number of inflammatory cells (mainly LYMs, neutrophils, macrophages, etc.), while the degree of fibroconnective tissue and of vascularisation were observed in or around the implant centre. The bone tissue formation in the Masson's trichrome staining was graded using an ordinal scoring system by the pathologist expert in scoring experimental animal tissue sections. At least three sections of each sample of excised animal tissue were read and evaluated. In this experiment, the degree of tissue inflammation was scored as 0 (normal or none); 1 (rarely seen); 2 (slightly increased, 5 to 20 per 40× field); or 3 (obviously increased, > 20/40× field). Bone regeneration was also evaluated and scored according to the degree of new bone formation as follows: 1, 2, 3, and 4 for none, rarely seen; ≤ 2/40× field, few or moderate; 3–10/40× field, and dense; > 10/40× field, respectively.

Bone structure analysis

The skull structure of the operated animals was analysed using micro-computed tomography (Micro CT, Skyscan1172, Antwerp, Belgium). The analysis conditions were 80 kV, 124 μA and resolution was 8 μm. Structural parameters of the skull were analysed using the built-in software. Total bone mineral density was measured, and the trabecular parameters of bone volume/total volume, trabecular number, trabecular pattern factor, and bone surface area per unit total volume were evaluated. Two-dimensional and 3D bone structure image slices were reconstructed.

Statistical analysis

Data are expressed as the mean ± standard deviation (SD). Differences between groups were analysed by one-way analysis of variance using GraphPad Prism 5 (GraphPad Software Inc., La Jolla, CA, USA) and Origin 6.1 (OriginLab Corporation, Northampton, MA, USA). A P value less than 0.05 was considered statistically significant.

Results

Description of animal behaviour

The skull defect surgery caused the OVX animals some weaknesses. The OVX animals with bone removed required a longer period to recover from the skull surgery with a longer period of persistent hair yellowing indicating the lack of self-cleaning and self-grooming activities. At 1–4 weeks after skull defect creation, the OVX animals showed some behavioural changes, with reduced drinking and eating compared to the normal rats. After week 4, all rats performed the same activities with no major differences between the groups. In general, the animals recovered from the surgery and the wounds healed within 10 weeks. Both OVX and normal rats with skull defects, however, exhibited a slight behavioural deviation with their heads occasionally rubbed into the bedding material. This behaviour continued up to the end of the experiment at 10 weeks post-operatively.

Routine blood tests in animals

Total blood counts were routinely performed in both OVX rats and normal rats in order to rule out any systemic effect from the treatments. Blood samples from each group of rats at 4 days and at 1, 2, 4 and 10 weeks were analysed. The parameters analysed included numbers of total white blood cells, haemoglobin, LYM, MPV, MON, neutrophils, platelets and red blood cells. In the control group, haemoglobin, neutrophil, red blood cell and white blood cell numbers were comparable between each type of material treatment and remained relatively constant across all time-points (**Figure 2**). There was no significant difference in the number of LYM between groups except for the result on day 4 showing lower number with the MeHA + TMV group. Slight increases of LYM were observed in all groups during the experimental period up to week 2. The number of MPV, MON and platelets showed no significant difference between the different groups. However, the MON count on day 4 showed a decrease in cell numbers in the group that was implanted with TMV-incorporated MeHA gel (MeHA + TMV). **Figure 3** shows the blood test results from OVX rats. Similar trends were observed across all types of blood cells. No significant differences were observed between treatment groups except for the LYM, MPV, and MON. The LYM and MON numbers from the TMV-incorporated MeHA gel were less than the other groups, a finding which was in agreement with the results observed in the normal rats. MPV showed significant reductions in the OVX rats treated with TMV-RGD-incorporated MeHA gel (MeHA + TMV-RGD). However, within 2 weeks, regular blood counts were restored in all rats in both control and OVX groups with no significant differences among any of the types of hydrogel treatment.

Hematoxylin and eosin staining of inflammatory cell infiltration

After 10 weeks, histological assessment of inflammatory cells around the implant sites revealed that inflammatory cell infiltration was significantly increased in the OVX rats in comparison to the normal rats with all types of hydrogel implant, but no difference was observed between the sham groups. Within the normal rats, MeHA + TMV-RGD treatment led to a significant reduction of inflammation around the implant site (mean score

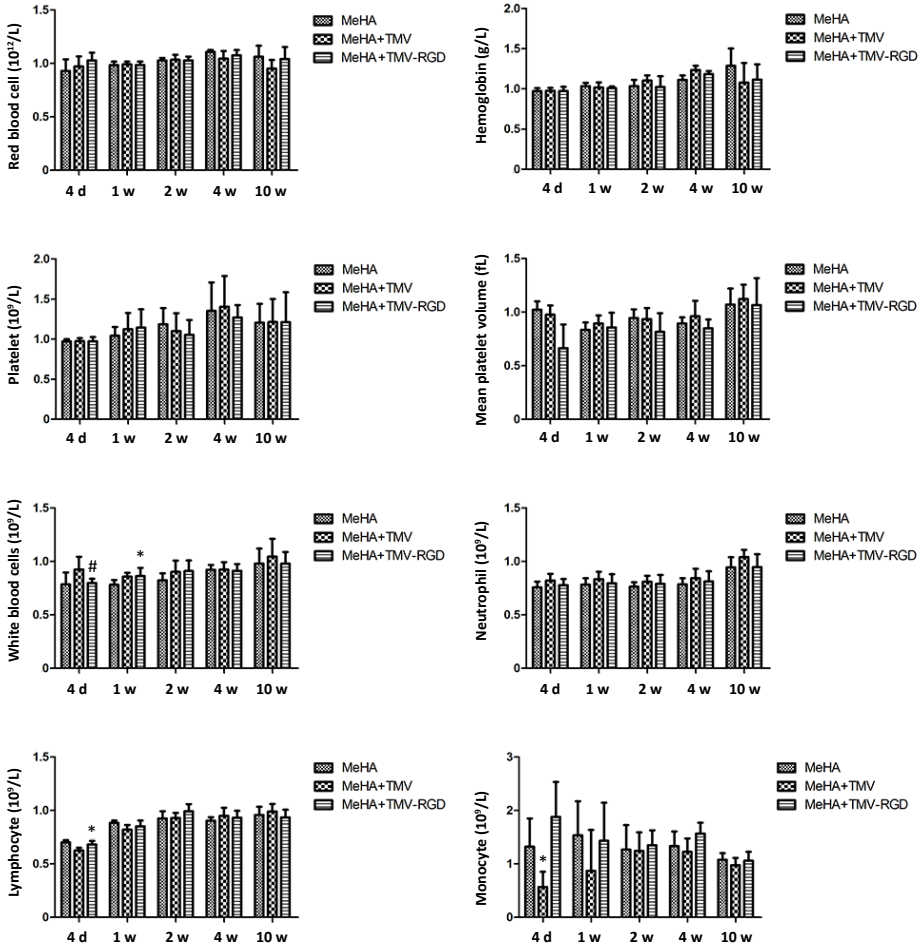

Figure 2. Haematological analysis of non-OVX animals treated with three different hydrogel materials (MeHA, MeHA + TMV, and MeHA + TMV-RGD) to fill their skull defects. Total blood counts were performed at five time points (4 days (d), 1, 2, 4, and 10 weeks (w)). Data are expressed as the mean ± SD (n = 3). *P < 0.05, *vs.* MeHA group; #P < 0.05, *vs.* MeHA + TMV group (one-way analysis of variance). MeHA: methacrylated hyaluronic acid; OVX: ovariectomised; RGD: arginyl-glycyl-aspartic acid; TMV: tobacco mosaic virus.

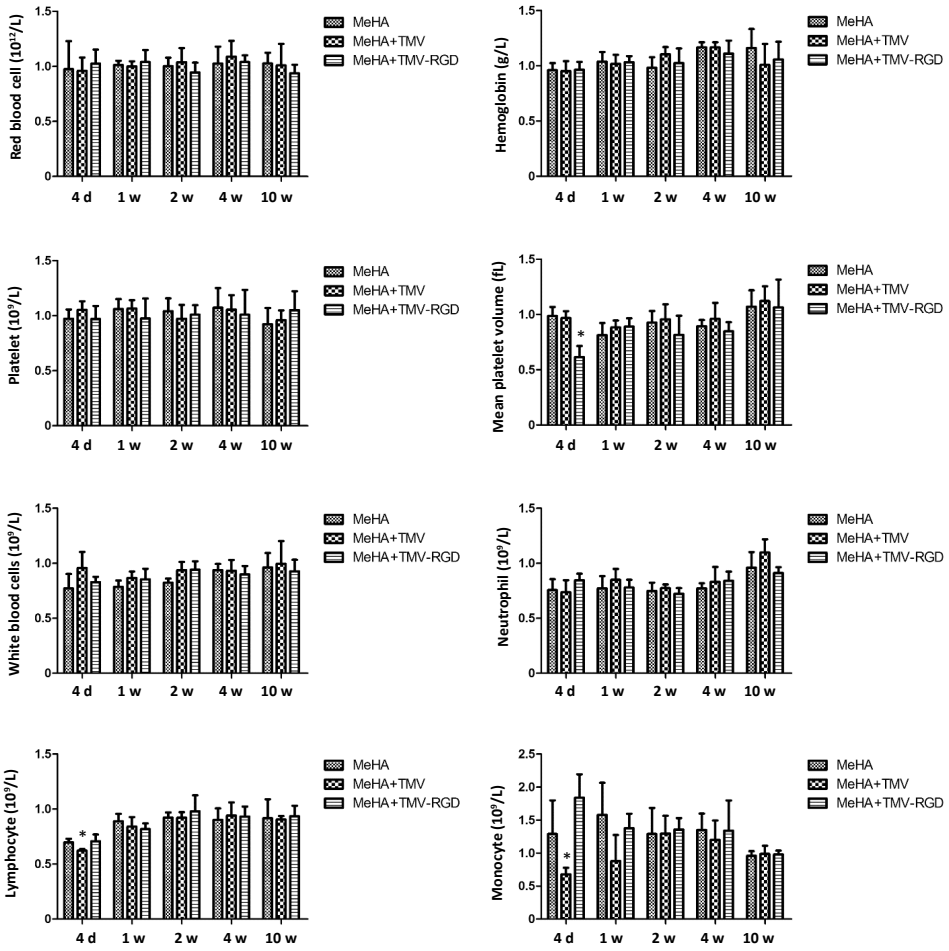

Figure 3. Haematological analysis of OVX animals treated with three different materials (MeHA, MeHA + TMV, and MeHA + TMV-RGD) to fill their skull defects. Total blood counts were performed at five time points (4 days (d), 1, 2, 4, and 10 weeks (w)). Data are expressed as the mean ± SD (n = 3). $^{**}P < 0.05$, *vs.* MeHA group (one-way analysis of variance). MeHA: methacrylated hyaluronic acid; OVX: ovariectomised; RGD: arginyl-glycyl-aspartic acid; TMV: tobacco mosaic virus.

for degree of inflammation = 0.8 ± 0.10), compared to the sham control without hydrogel (MeHA) and the MeHA + TMV groups (average score = 1.2 ± 0.25, 1.5 ± 0.15, and 1.3 ± 0.10, respectively). For the OVX rats, the minimal inflammation score of 1.3 ± 0.06 was also observed in the MeHA + TMV-RGD treatment groups while the MeHA and MeHA + TMV groups showed significantly higher inflammation scores (average score = 2.5 ± 0.10 and 2.7 ± 0.31, respectively) compared to the sham control (1.6 ± 0.15). Interestingly, these results suggest that TMV-RGD could compromise the local inflammatory response caused by the surgical skull defect. These data show that neither the virus incorporated into the hydrogel nor the hydrogel itself induced excessive inflammation or any adverse tissue reactions in the rat cranial defect model.

Bone healing was also evaluated in the H&E-stained sections (**Figure 4**). The void spots in the histological sections represented the defect area without any new tissue formation, and their sizes were calculated as a percentage of the bone healing area. **Figure 4** shows significant increases in the area of bone tissue formation from all types of implants in the normal rats, with the highest score given to the group with implanted TMV-RGD (mean score = 0.5 ± 0.06), followed by the TMV (mean score = 0.3 ± 0.04), and the blank MeHA hydrogel (mean score = 0.1 ± 0.02). The same trend was also observed in the OVX model, with the most intense bone tissue formation scoring a mean of 0.3 ± 0.02 for the sections from TMV-RGD MeHA hydrogel-implanted rats. Overall, the bone formation scores given to each type of implant were significantly lower in the OVX rats compared to the normal groups. This is expected because OVX causes impaired bone regeneration. Altogether, both evaluations from H&E staining indicated that all types of hydrogels had a positive effect in inducing bone formation, with the TMV-RGD hydrogel implant having the greatest bone induction potential and the best *in vivo* compatibility.

Masson's trichrome staining

Masson's trichrome staining was used to confirm the results of H&E staining in terms of bone tissue regeneration potential induced by the implanted hydrogels in the cranial defects of rats in both control and OVX groups at 10 weeks post-surgery to identify the amount of new calcified bone in the defect area.

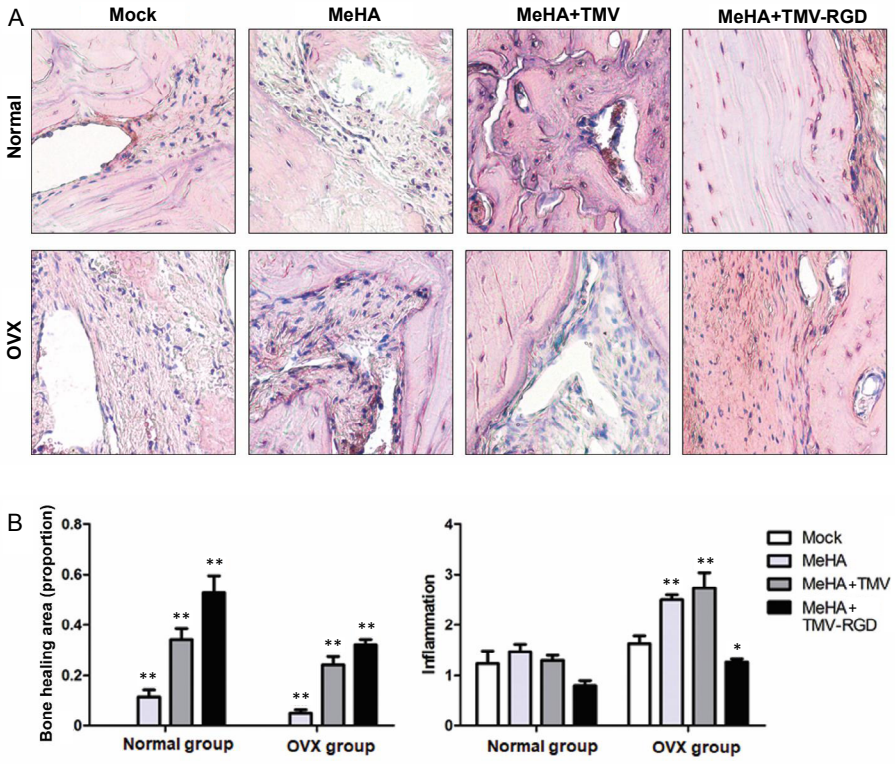

Figure 4. Inflammatory cell infiltration observed by hematoxylin and eosin staining. (A) Photomicrographs of hematoxylin and eosin-stained sections from skull defects implanted with each type of hydrogel (MeHA, MeHA + TMV, and MeHA + TMV-RGD) (original magnification, 40×). The new bone is visible as a compact structure with a pink colour. The connective tissue can be seen as a structured network of cells in a purple colour. (B) Hematoxylin and eosin histological scoring of the three types of hydrogels confirm the difference in proportion of bone healing area and degree of inflammation (arbitrary scoring). Data are expressed as the mean ± SD (n = 3). *P < 0.05, **P < 0.01, *vs.* sham group (one-way analysis of variance). MeHA: methacrylated hyaluronic acid; OVX: ovariectomised; RGD: arginyl-glycyl-aspartic acid; TMV: tobacco mosaic virus.

As shown in **Figure 5A**, no or only minimal new bone was observed in the control group at 10 weeks post-surgery, especially in the OVX rat group. The degree of bone injury in the OVX group was more serious than that in the normal group. In both rat models, the formation of new bone in the defect area treated with any of the three types of MeHA-based hydrogel was pronounced. The sham groups showed highly intense blue staining with less red stain indicating lower density of bone tissue. Consistent with H&E analysis, all three implant materials showed increased red staining, among which the TMV-RGD material group had the most intense red stain, indicating remarkably increased bone tissue repair.

Figure 5B shows the mean scores corresponding to the mature bone area observed in the implanted groups when normalised to the sham group within each particular model. The same trend was shared between the two animal models (normal and OVX) with the highest bone formation in the TMV-RGD MeHA implant group. However, the OVX rats appeared to show only a minimal response towards all treatments as expected.

The skull defect area from each treatment group, in both control and OVX rats, was subjected to micro-CT. In the normal rats, the treatment groups showed slight differences in the area of the defect, correlating with the histological score.

As shown in **Figure 5C**, the unmodified hydrogel induced minimal growth from the circular edge of the defect over the calvarial CSDs in the sham control rats, since intramembranous bone formation starts only from the defect margins and progresses centripetally to eventually fill the original defect.[30] The penetration of new bone tissue formation into the CSDs seemed to be enhanced progressively in respect to the hydrogel implants with TMV and TMV-RGD1. However, with the induction of osteoporosis by OVX, micro-CT analysis showed no observable regenerated hard bone structure in response to any treatments within the observation period. A possible explanation is that the 10-week implantation period before animal sacrifice was not long enough to allow the complete formation of calcified hard bone tissue due to compromised performance of bone regeneration in the model animals. A previous study demonstrated significant impairment of the amount of newly-formed bone observed in OVX animals at three and six months of healing, compared with the sham-operated animals.[31] This could indicate that the critical period for observable healing would need to be longer after OVX. In addition, the experimental challenge for bone defects used in this study involved the combination of creation of a defect (calvarial CSD) and osteoporosis induction. A pre-clinical report from OVX animals demonstrated that osteoporosis may reduce bone mechanical properties and retard post-fracture bone healing.[32, 33]

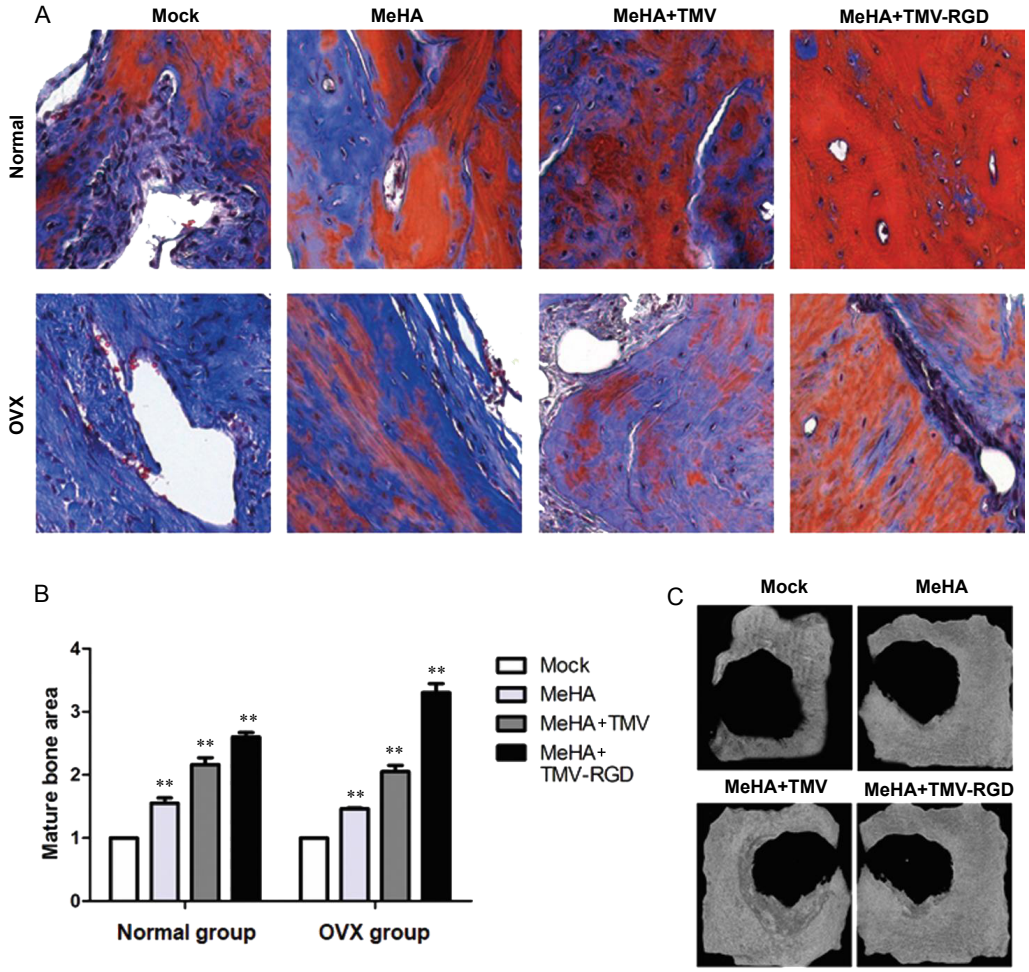

Figure 5. Histopathological analysis of bone substitute hydrogel implants stained with Masson's trichrome. (A) Photomicrographs of corresponding Masson's trichrome-stained sections from each type of hydrogel (original magnification, 40×). In general, Masson's trichrome stains mature bone with osteoid formation red, whilst blue stain indicates developing calcified bone. (B) Histological scoring of the three types of hydrogels in tissue sections show the different amounts of mature bone area. Data are expressed as the mean ± SD (n = 3). *P < 0.05, **P < 0.01, *vs.* sham group (one-way analysis of variance). (C) Micro CT images of the cranial-defected bones dissected from non-OVX groups with different types of hydrogel implants at 10 weeks post-surgery. MeHA: methacrylated hyaluronic acid; OVX: ovariectomised; RGD: arginyl-glycyl-aspartic acid; TMV: tobacco mosaic virus.

Reduced bone formation and lower bone quality have also been reported in grafted bony defects, in calvarial CSDs treated with guided bone regeneration and a graft.[31, 34] As calvarial CSDs are known to be relatively more challenging compared to other research models, for example, infrabony or alveolar defects, where all the bony surfaces surrounding the defects may facilitate the regeneration process and act as a reservoir of osteoprogenitor cells,[30] this may have been responsible for the low levels of bone regeneration observed in our study.

Discussion

This study was designed to investigate two major aspects. First, to produce proof-of-concept findings regarding whether the cellular response towards TMV could be implemented under physiological conditions. This study was considered part of the continuing effort to emphasise the concept of utilising plant viruses in the biomaterial platform to innovate molecular designs featuring the material's nanostructure for application in tissue regeneration by manipulation of cell interactions to induce a cellular response. Second, the experiment was designed as a step closer towards medical use of the plant virus in the hydrogel platform for regenerative medicine, for the treatment of tissue damage that could arise due to aging or trauma. The materials were used as cranial defect bone fillers and were tested in both normal rats as well as in an osteoporosis model. The result showed that bone healing was induced by the hydrogel scaffolds modified with TMV or with the TMV-RGD mutant. Bone formation was enhanced by incorporation of the RGD peptide onto the surface of the TMV particle by genetic modification of TMV. This virus-functionalisation approach could potentially be a method of choice for the modification of biocompatible materials used in biomedical treatments.

Author contributions

Conceptualisation: JYuan, JAL; methodology: JYuan, JAL, PM; software: JYuan, ZZ, BL, JYang; validation: ZZ, BL, YL; formal analysis, data curation, and writing—original draft preparation: JYuan, JAL;

investigation: JYuan, JYang, PM; resources: JYuan, JAL; writing—review and editing, YL, PM; visualisation: JAL, PM; supervision: JAL; project administration:, JYuan, ZZ, BL, JYang; funding acquisition: JYuan, YL, JAL. All authors have read and agreed to the published version of the manuscript.

Financial support

This research was supported by the Thailand Research Fund and Office of the Higher Education Commission (No. MRG6180264), Chulalongkorn University, and the National Natural Science Foundation of China (No. 21750110445).

Acknowledgement

The corresponding author (JAL) would like to thank Professor Prasit Pavasant, Faculty of Dentistry at Chulalongkorn University, for his advice. All authors would like to thank Professor Zhaohui Su for the access to instruments and facilities used in this research at Changchun Institute of Applied Chemistry (CIAC), Changchun, China. Graphical abstract and Figure 1 were Created with BioRender.com.

Conflicts of interest statement

The authors declare no conflict of interest.

1. Kaur, G.; Valarmathi, M. T.; Potts, J. D.; Jabbari, E.; Sabo-Attwood, T.; Wang, Q. Regulation of osteogenic differentiation of rat bone marrow stromal cells on 2D nanorod substrates. *Biomaterials.* **2010**, *31*, 1732-1741.
2. Kaur, G.; Wang, C.; Sun, J.; Wang, Q. The synergistic effects of multivalent ligand display and nanotopography on osteogenic differentiation of rat bone marrow stem cells. *Biomaterials.* **2010**, *31*, 5813-5824.
3. Maturavongsadit, P.; Luckanagul, J. A.; Metavarayuth, K.; Zhao, X.; Chen, L.; Lin, Y.; Wang, Q. Promotion of in vitro chondrogenesis of mesenchymal stem cells using in situ hyaluronic hydrogel functionalized with rod-like viral nanoparticles. *Biomacromolecules.* **2016**, *17*, 1930-1938.
4. Metavarayuth, K.; Sitasuwan, P.; Luckanagul, J. A.; Feng, S.; Wang, Q. Virus nanoparticles mediated osteogenic differentiation of bone derived mesenchymal stem cells. *Adv Sci (Weinh).* **2015**, *2*, 1500026.
5. Sitasuwan, P.; Lee, L. A.; Bo, P.; Davis, E. N.; Lin, Y.; Wang, Q. A plant virus substrate induces early upregulation of BMP2 for rapid bone formation. *Integr Biol (Camb).* **2012**, *4*, 651-660.
6. Zhao, X.; Lin, Y.; Wang, Q. Virus-based scaffolds for tissue engineering applications. *Wiley Interdiscip Rev Nanomed Nanobiotechnol.* **2015**, *7*, 534-547.
7. Nguyen, H. G.; Metavarayuth, K.; Wang, Q. Upregulation of osteogenesis of mesenchymal stem cells with virus-based thin films. *Nanotheranostics.* **2018**, *2*, 42-58.
8. Griffith, L. G.; Naughton, G. Tissue engineering--current challenges and expanding opportunities. *Science.* **2002**, *295*, 1009-1014.
9. Khademhosseini, A.; Langer, R.; Borenstein, J.; Vacanti, J. P. Microscale technologies for tissue engineering and biology. *Proc Natl Acad Sci U S A.* **2006**, *103*, 2480-2487.
10. Khademhosseini, A.; Vacanti, J. P.; Langer, R. Progress in tissue engineering. *Sci Am.* **2009**, *300*, 64-71.
11. Khademhosseini, A.; Langer, R. Microengineered hydrogels for tissue engineering. *Biomaterials.* **2007**, *28*, 5087-5092.
12. Zhu, J. Bioactive modification of poly(ethylene glycol) hydrogels for tissue engineering. *Biomaterials.* **2010**, *31*, 4639-4656.
13. Bichara, D. A.; Zhao, X.; Bodugoz-Senturk, H.; Ballyns, F. P.; Oral, E.; Randolph, M. A.; Bonassar, L. J.; Gill, T. J.; Muratoglu, O. K. Porous poly(vinyl alcohol)-hydrogel matrix-engineered biosynthetic cartilage. *Tissue Eng Part A.* **2011**, *17*, 301-309.
14. Elisseeff, J. Injectable cartilage tissue engineering. *Expert Opin Biol Ther.* **2004**, *4*, 1849-1859.
15. Aldaye, F. A.; Senapedis, W. T.; Silver, P. A.; Way, J. C. A structurally tunable DNA-based extracellular matrix. *J Am Chem Soc.* **2010**, *132*, 14727-14729.
16. Kloxin, A. M.; Kasko, A. M.; Salinas, C. N.; Anseth, K. S. Photodegradable hydrogels for dynamic tuning of physical and chemical properties. *Science.* **2009**, *324*, 59-63.
17. Luckanagul, J.; Lee, L. A.; Nguyen, Q. L.; Sitasuwan, P.; Yang, X.; Shazly, T.; Wang, Q. Porous alginate hydrogel functionalized with virus as three-dimensional scaffolds for bone differentiation. *Biomacromolecules.* **2012**, *13*, 3949-3958.
18. Luckanagul, J. A.; Lee, L. A.; You, S.; Yang, X.; Wang, Q. Plant virus incorporated hydrogels as scaffolds for tissue engineering possess low immunogenicity in vivo. *J Biomed Mater Res A.* **2015**, *103*, 887-895.
19. Luckanagul, J. A.; Metavarayuth, K.; Feng, S.; Maneesaay, P.; Clark, A. Y.; Yang, X.; García, A. J.; Wang, Q. Tobacco mosaic virus functionalized alginate hydrogel scaffolds for bone regeneration in rats with cranial defect. *ACS Biomater Sci Eng.* **2016**, *2*, 606-615.
20. Mahajan, H. S.; Gattani, S. In situ gels of Metoclopramide Hydrochloride for intranasal delivery: in vitro evaluation and in vivo pharmacokinetic study in rabbits. *Drug Deliv.* **2010**, *17*, 19-27.
21. Burdick, J. A.; Prestwich, G. D. Hyaluronic acid hydrogels for biomedical applications. *Adv Mater.* **2011**, *23*, H41-56.
22. Maturavongsadit, P.; Bi, X.; Metavarayuth, K.; Luckanagul, J. A.; Wang, Q. Influence of cross-linkers on the in vitro chondrogenesis of mesenchymal stem cells in hyaluronic acid hydrogels. *ACS Appl Mater Interfaces.* **2017**, *9*, 3318-3329.
23. Ananthanarayanan, B.; Kim, Y.; Kumar, S. Elucidating the mechanobiology of malignant brain tumors using a brain matrix-mimetic hyaluronic acid hydrogel platform. *Biomaterials.* **2011**, *32*, 7913-7923.
24. Jakob, F.; Ebert, R.; Ignatius, A.; Matsushita, T.; Watanabe, Y.; Groll, J.; Walles, H. Bone tissue engineering in osteoporosis. *Maturitas.* **2013**, *75*, 118-124.
25. Lelovas, P. P.; Xanthos, T. T.; Thoma, S. E.; Lyritis, G. P.; Dontas, I. A. The laboratory rat as an animal model for osteoporosis research. *Comp Med.* **2008**, *58*, 424-430.
26. Wronski, T. J.; Cintrón, M.; Dann, L. M. Temporal relationship between bone loss and increased bone turnover in ovariectomized rats. *Calcif Tissue Int.* **1988**, *43*, 179-183.
27. Wronski, T. J.; Dann, L. M.; Scott, K. S.; Cintrón, M. Long-term effects of ovariectomy and aging on the rat skeleton. *Calcif Tissue Int.* **1989**, *45*, 360-366.
28. Xin, Z.; Jin, C.; Chao, L.; Zheng, Z.; Liehu, C.; Panpan, P.; Weizong, W.; Xiao, Z.; Qingjie, Z.; Honggang, H.; Longjuan, Q.; Xiao, C.; Jiacan, S. A matrine derivative M54 suppresses osteoclastogenesis and prevents ovariectomy-induced bone loss by targeting ribosomal protein S5. *Front Pharmacol.* **2018**, *9*, 22.
29. Zhou, L.; Liu, Q.; Yang, M.; Wang, T.; Yao, J.; Cheng, J.; Yuan, J.; Lin, X.; Zhao, J.; Tickner, J.; Xu, J. Dihydroartemisinin, an anti-malaria drug, suppresses estrogen deficiency-induced osteoporosis, osteoclast formation, and RANKL-induced signaling pathways. *J Bone Miner Res.* **2016**, *31*, 964-974.
30. Mardas, N.; Stavropoulos, A.; Karring, T. Calvarial bone regeneration by a combination of natural anorganic bovine-derived hydroxyapatite matrix

coupled with a synthetic cell-binding peptide (PepGen): an experimental study in rats. *Clin Oral Implants Res.* **2008**, *19*, 1010-1015.

31. Durão, S. F.; Gomes, P. S.; Colaço, B. J.; Silva, J. C.; Fonseca, H. M.; Duarte, J. R.; Felino, A. C.; Fernandes, M. H. The biomaterial-mediated healing of critical size bone defects in the ovariectomized rat. *Osteoporos Int.* **2014**, *25*, 1535-1545.
32. Namkung-Matthai, H.; Appleyard, R.; Jansen, J.; Hao Lin, J.; Maastricht, S.; Swain, M.; Mason, R. S.; Murrell, G. A.; Diwan, A. D.; Diamond, T. Osteoporosis influences the early period of fracture healing in a rat osteoporotic model. *Bone.* **2001**, *28*, 80-86.
33. Hao, Y. J.; Zhang, G.; Wang, Y. S.; Qin, L.; Hung, W. Y.; Leung, K.; Pei, F. X. Changes of microstructure and mineralized tissue in the middle and late phase of osteoporotic fracture healing in rats. *Bone.* **2007**, *41*, 631-638.
34. Oberg, S.; Johansson, C.; Rosenquist, J. B. Bone formation after implantation of autolysed antigen extracted allogeneic bone in ovariectomized rabbits. *Int J Oral Maxillofac Surg.* **2003**, *32*, 628-632.

Received: September 11, 2020
Revised: October 13, 2020
Accepted: October 14, 2020
Available online: December 28, 2020